microbial biotechnology

Open Access

Role of phenazine-enzyme physiology for current generation in a bioelectrochemical system

Anthony Chukwubuikem,[1,2] Carola Berger,[2] Ahmed Mady[2] and Miriam A. Rosenbaum[1,2]

[1]*Bio Pilot Plant, Leibniz Institute for Natural Product Research and Infection Biology – Hans-Knöll-Institute (HKI), Jena, Germany.*

[2]*Faculty of Biological Sciences, Friedrich Schiller University (FSU), Jena, Germany.*

Summary

Pseudomonas aeruginosa **produces phenazine-1-carboxylic acid (PCA) and pyocyanin (PYO), which aid its anaerobic survival by mediating electron transfer to distant oxygen. These natural secondary metabolites are being explored in biotechnology to mediate electron transfer to the anode of bioelectrochemical systems. A major challenge is that only a small fraction of electrons from microbial substrate conversion is recovered. It remained unclear whether phenazines can re-enter the cell and thus, if the electrons accessed by the phenazines arise mainly from cytoplasmic or periplasmic pathways. Here, we prove that the periplasmic glucose dehydrogenase (Gcd) of *P. aeruginosa* and *P. putida* is involved in the reduction of natural phenazines. PYO displayed a 60-fold faster enzymatic reduction than PCA; PCA was, however, more stable for long-term electron shuttling to the anode. Evaluation of a Gcd knockout and overexpression strain showed that up to 9% of the anodic current can be designated to this enzymatic reaction. We further assessed phenazine uptake with the aid of two molecular biosensors, which experimentally confirm the phenazines' ability to re-enter the cytoplasm. These findings significantly advance the understanding of the (electro) physiology of phenazines for future tailoring of phenazine electron discharge in biotechnological applications.**

Received 12 March, 2021; revised 14 April, 2021; accepted 27 April, 2021.

For correspondence. E-mail miriam.rosenbaum@leibniz-hki.de; Tel. (+49)3641 5321120; Fax (+49) 3641 5320805.

Microbial Biotechnology (2021) **14**(4), 1613–1626
doi:10.1111/1751-7915.13827

Introduction

Energy is the key factor, which drives metabolism in all organisms (Alexandre *et al*., 2004). Microorganisms produce energy in the form of ATP mainly by the systematic transfer of electrons through their electron transport chains to a terminal electron acceptor such as oxygen, nitrate or sulphate (Kracke *et al*., 2015; Kuypers *et al*., 2018). Electroactive microorganisms are in addition able to transport electrons through their cellular membrane to the extracellular environment to reduce solid-state electron acceptors such as Fe(III) and Mn(IV) (Kato, 2015; Shi *et al*., 2016). This discharge of electrons can be harnessed in a bioelectrochemical system (BES), where electrons are channelled to an electrode (anode) as an alternative electron acceptor (Pant *et al*., 2012; Logan *et al*., 2019). BES technology currently holds potentials in various fields, the most renowned being the microbial fuel cell (MFC) used for wastewater treatment (Pandey *et al*., 2016). Additionally, a fairly new field applies BES in biotechnology for new oxygen-limited bioprocesses, as they can provide an oxygen-independent alternative for discharging excess electrons and thereby maintaining the metabolic flux of the organism (Schmitz *et al*., 2015; Askitosari, 2019).

Electrons are transferred to the electrodes of a BES either by direct contact of the microorganisms or by using soluble redox mediators (Shi *et al*., 2016, Beblawy *et al*., 2018; Lovley and Walker, 2019; Saunders *et al*., 2020). For biotechnological applications, the use of the latter has several advantages. Redox mediators are in principle non-exhaustible (Brutinel and Gralnick, 2012) and based on the three-dimensional culture broth, there is no limit to the extent mediators can travel. This is in contrast to direct electron transfer, which is limited to the 2D surface area of the electrode. The natural mediators produced by *Pseudomonas aeruginosa* are termed phenazines, with phenazine-1-carboxylic acid (PCA) and pyocyanin (PYO) being the ones dominantly produced (Mavrodi *et al*., 2001). Although these colourful secondary metabolites are mostly known for the different roles they play as a pathogenicity factor in *P. aeruginosa* infections (Hall *et al*., 2016; Yang *et al*., 2016), they also have been shown to enhance the anaerobic survival of the organism by shuttling electrons to distant oxygen (Wang *et al*., 2010). Phenazines may receive electrons from NAD(P)H, as shown *in vitro*, and from some

cytoplasmic enzymatic conversions of central metabolic pathways (Price-Whelan *et al*., 2007; Glasser *et al*., 2017; Jo *et al*., 2020). Reduced phenazines mediate these electrons to distant oxygen or other feasible electron acceptors such as the anode of a BES and with this, enable the survival of *P. aeruginosa* in an oxygen-limited environment (Pham *et al*., 2008; Glasser *et al*., 2014). Recently, biotechnologically important strains such as *P. putida* KT2440 and *E. coli* have been engineered to produce these phenazines, thereby boosting the prospects of using these redox-active compounds for electron transfer in electrochemical bioprocesses (Schmitz *et al*., 2015; Feng *et al*., 2018; da Silva et al., 2021).

However, the energetic use of phenazines for electron discharge, both in native and biotechnologically relevant *Pseudomonas* species, is limited, and only a small fraction of electrons provided by the substrate, for example glucose, is discharged to the extracellular electron acceptor (Bosire *et al*., 2016). Additionally, this electron discharge currently does not seem to directly yield ATP for the cell (Glasser *et al*., 2014). Since phenazine biosynthesis and all identified phenazine reduction pathways occur in the cytoplasm (Blankenfeldt and Parsons, 2014; Glasser *et al*., 2017; Jo *et al*., 2020), a central question is if phenazines can in fact re-enter the cell once they have been pumped outside. This has not been experimentally verified yet, but is a requirement to enable a potentially broader enzymatic reduction. We here hypothesize that a significant part of the phenazine reduction takes place already in the periplasm (Fig. 1) and tested this hypothesis with two approaches: (i) specific phenazine reduction by periplasmic reductases and (ii) the development of bioassays to verify phenazine entry into the cytosol.

Pseudomonas species commonly utilize glucose via a direct glucose oxidation pathway, which occurs in the periplasm (Daddaoua *et al*., 2010; Kohlstedt and Wittmann, 2019). This pathway involves the oxidation of glucose to 2-ketogluconic acid via gluconate, and both sugar acids are commonly found as accumulated intermediates in *Pseudomonas* BES cultivations (Schmitz *et al*., 2015; Bosire *et al*., 2016). The first step of this reaction, the oxidation of glucose to gluconate, is catalysed by a membrane-bound pyrroloquinoline quinone (PQQ)-dependent glucose dehydrogenase (Gcd), which transfers two electrons via PQQ to ubiquinone, localized in the membrane and eventually to the electron transport chain (Van Schie *et al*., 1985; Kobayashi *et al*., 2005). Here, we evaluate this enzyme for its capacity of phenazines reduction.

To assay the uptake of phenazines into the cytosol, we developed two molecular biosensors. One of them utilized the fact that PYO is synthesized intracellularly from PCA as a precursor (Mentel *et al*., 2009). We provided external PCA to a strain exclusively harbouring the genes to turn PCA into PYO, and measured the cytoplasmic transformation into PYO. The second biosensor tracked PYO access to the cell by harnessing the ability of endogenous phenazines to oxidize the (2Fe-2S) transcription factor SoxR, which in turn activates the promoter of the MexGHI-OpmD efflux pump operon involved in phenazine export (Palma *et al*., 2005; Dietrich *et al*., 2006; Sakhtah *et al*., 2016).

Results

To test our first hypothesis that phenazine reduction can take place in the periplasm, we evaluated the interaction of the phenazines with the first enzyme of the periplasmic glucose oxidation pathway *in vitro* and *in vivo*.

Membrane-bound glucose dehydrogenase (Gcd) of Pseudomonas *reduces phenazines* in vitro

We first tested, if phenazines could interact with the membrane-bound glucose dehydrogenase (Gcd) of *Pseudomonas* and as such mediate the electrons generated through the oxidation of glucose in the periplasmic space to extracellular terminal electron acceptors. The *gcd* genes of *P. aeruginosa* PA14 (PA14_34970) and *P. putida* KT2440 (PP_1444) were cloned and expressed in *E. coli*. Both proteins, each made up of 803 amino acid residues, are PQQ-dependent and require divalent ions such as calcium ions as an enhancing co-factor. The initial 138 to 140 amino acids at the N-terminus form a membrane anchor with five transmembrane helices, while the remaining part of the protein, including the catalytic site, flanks the periplasmic space. The final construct of the Gcds used for protein expression contained C- and N-terminal His-tag sequences and excluded the first 8 native amino acids, since the construct with the full native sequence showed retarded growth and a low protein expression. The membrane proteins were purified for the enzyme assay using affinity and size permeation chromatography (Fig. S1).

If the Gcds can interact with phenazines, they should be able to reduce these mediators by transferring electrons from the glucose oxidation through the PQQ co-factor to the phenazines (Fig. 1). An enzyme assay was performed with the purified proteins using PCA and PYO as prospective electron acceptors. The standard electron acceptors of an established dehydrogenase enzyme assay (Jahn *et al*., 2020), phenazine methanosulfate (PMS) and dichlorophenolindophenol (DCPIP), were used as control reaction to verify activity of the enzyme. When either PCA or PYO was used as electron acceptor in this reaction, the Gcd of *P. aeruginosa* PA14 was able

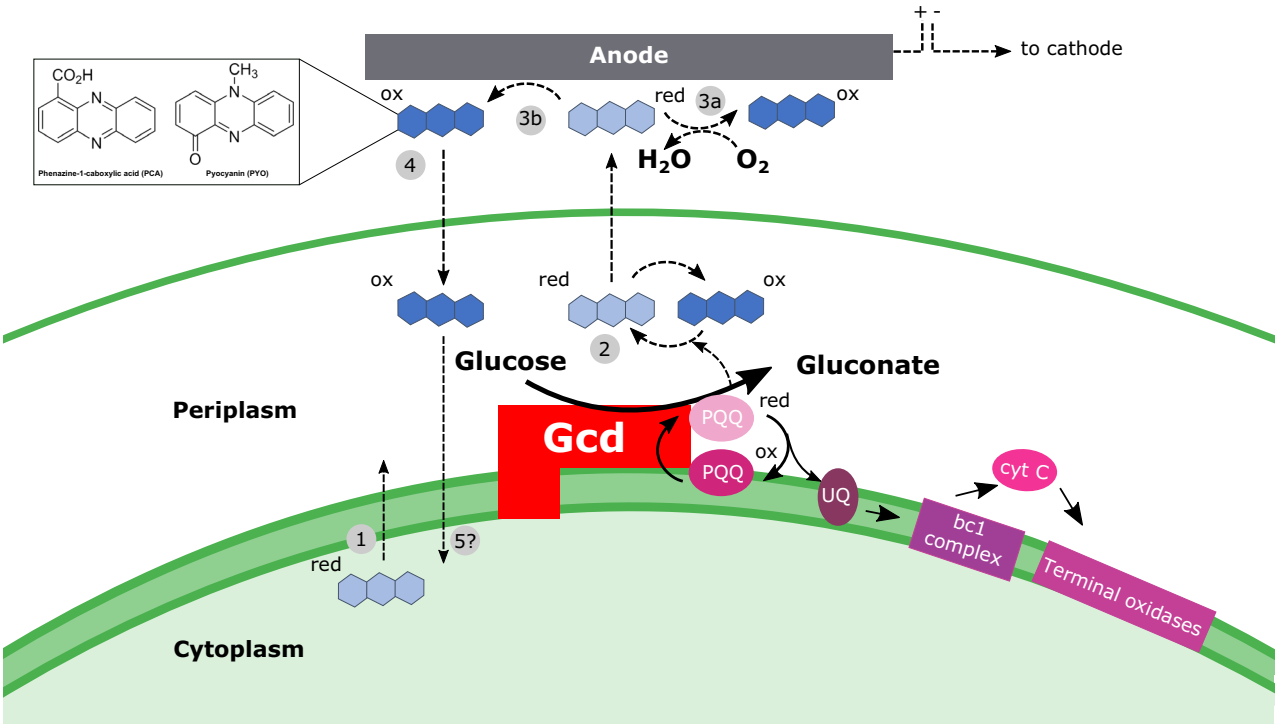

Fig. 1. Oxidation of glucose to gluconate by the membrane-bound periplasmic glucose dehydrogenase (Gcd). The solid arrows show the conventional flow of electrons generated in this oxidation via pyrroloquinolone quinone (PQQ) to ubiquinone (UQ) and further to the electron transport chain at the level of ubiquinone and cytochrome c (cyt c). The dotted arrows depict all phenazine-related transfer or reaction pathways: Phenazines (aromatic rings) produced in the cytoplasm (1) or exogenously added accept electrons through PQQ (2). These electrons are used for oxygen reduction (3a) or are mediated to the anode of a BES for generation of electrical current (3b). Oxidized phenazines subsequently re-enter the periplasm to continue the cycle (4) although it is not clear if and how it re-enters the cytoplasm (5?). Insert: Two main phenazines produced by *P. aeruginosa*, phenazine-1-carboxylic acid (PCA) and pyocyanin (PYO).

to catalyse the transfer of electrons from glucose to these phenazines, which resulted in their measurable reduction (Fig. 2A and B). A control in which water was used to replace either the substrate or the enzyme did not show any phenazine reduction. We also performed the same assay with Gcd obtained from *P. putida* KT2440, a prospective organism for limited-oxygen BES processes (Askitosari *et al.*, 2019). Comparison of the Gcds of *P. aeruginosa* PA14 and *P. putida* KT2440 showed 81.64% and 78.93% sequence identities in their nucleotide and amino acid sequences respectively. The enzyme assay with the Gcd of *P. putida* KT2440 equally showed reduction of PCA and PYO utilizing electrons from glucose oxidation (Fig. 2C and D). No reduction of the phenazines was observed for both enzymes when PQQ or calcium ions were excluded from the reaction (results not shown). The reduction rate of PYO was about 60 times faster than that of PCA for both Gcds (Fig. 2). The experiments clearly confirmed the membrane-bound glucose dehydrogenases of *P. aeruginosa* and *P. putida* as potential phenazine reducing enzymes.

Confirming Gcd-phenazine reduction in vivo *using bioelectrochemical system (BES)*

Having established that a periplasmic enzyme can interact with phenazines, we tested if this is a major pathway for phenazine reduction *in vivo*. To ascertain the proportion of electrons generated from the periplasmic glucose oxidation pathway versus downstream cytoplasmic pathways, a BES was set up using three *Pseudomonas putida* KT2440 strains: a wild-type strain (KT2440 wt), a glucose dehydrogenase deletion mutant (KT2440 Δ*gcd*), in which the native Gcd was removed, and an overexpression strain, which was supplied with a plasmid for expressing the glucose dehydrogenase of *P. aeruginosa* PA14 (KT2440 Δ*gcd*–PA14*gcd*). The Gcd of PA14 was used for the overexpression because PA14 is a natural producer of phenazines and had an overall better performance in the enzyme assay (Fig. 2). The wild-type and overexpression strains are able to metabolize glucose using the periplasmic as well as the cytoplasmic pathways, while the Gcd mutant strain can only use the cytoplasmic pathway. PCA (80 mg l^{-1}) or PYO (18 mg l^{-1})

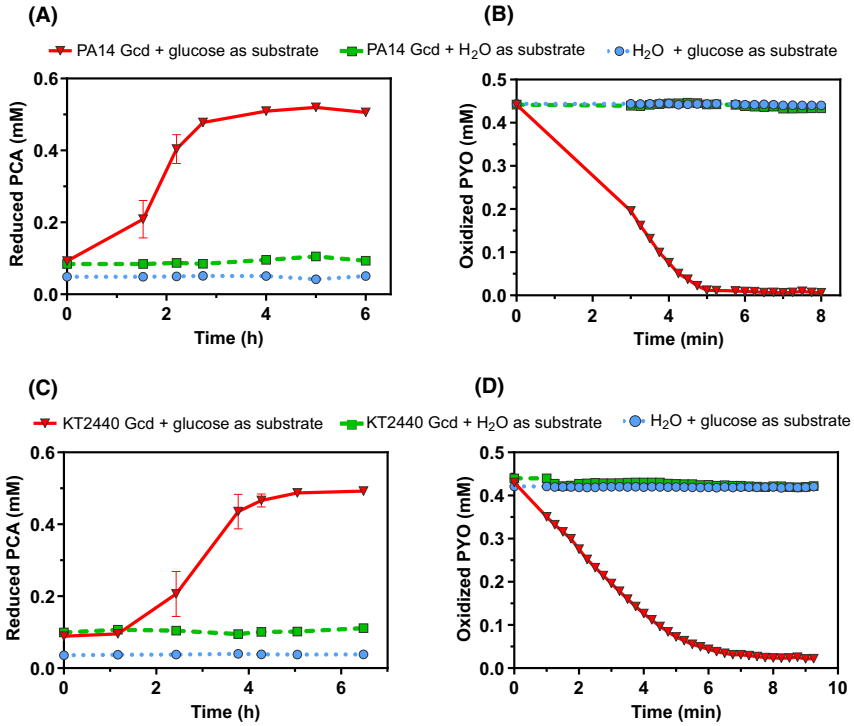

Fig. 2. Phenazine reduction by periplasmic membrane-bound PQQ-dependent glucose dehydrogenase (Gcd) of *P. aeruginosa* PA14 (PA14 Gcd) and *P. putida* KT2440 (KT2440 Gcd).
A. increase in concentration of reduced phenazine-1-carboxylic acid (PCA) and (B) decrease in concentration of oxidized pyocyanin (PYO) by the interaction with PA14 Gcd; (C) increase in concentration of reduced PCA and (D) decrease in concentration of oxidized PYO by the interaction with KT2440 Gcd. To measure the phenazines, decrease in the absorbance of oxidized PYO was followed at 690 nm and the concentration (mM) was calculated using an extinction coefficient of 4.5 $mM^{-1}cm^{-1}$, while the formation of the reduced PCA was followed at 440 nm and the concentration (mM) was calculated using an extinction coefficient of 2.05 $mM^{-1}cm^{-1}$. The reaction mixture contained in 200 µl: 100 mM Tris-HCl pH 7.0, 1 mM $CaCl_2$, 0.45 mM of the phenazines, 65 µg ml^{-1} enzyme or water, 5 µM PQQ and 20 mM glucose or water was used to complete the reaction. Results show the average of three replicates; error bars indicate standard deviation (SD).

were added to the system 23 h after inoculation (time point 'a' in Fig. 3A and B). A higher concentration of PCA was used because it showed a lower Gcd reduction rate (Fig. 2) and to be in consistency with the amounts typically produced by *Pseudomonas* in a BES (Askitosari *et al.*, 2019). As expected, no electrons were discharged to the anode during the active aeration growth period (first 31 h) as electrons from glucose oxidation were preferably moved to oxygen (Fig. 3A and B).

The current, however, increased for the three strains once the supply of oxygen was turned off (passive aeration, time point 'b' in Fig. 3A and B), indicating that phenazines mediated electrons to the anode (Fig. 3A and B). The KT2440 Δ*gcd*–PA14 *gcd* strain attained the highest maximum current density (25.9 µA cm^{-2}) in the PCA-BES, which was a 55% and 63% increase compared to the KT2440 wt and the KT2440 Δ*gcd* respectively (Fig. 3A). Similarly, in the PYO-BES, KT2440 Δ*gcd*–PA14 *gcd* had a peak current density of 12.2 µA cm^{-2}, while the KT2440 wt and KT2440 Δ*gcd* showed a maximum of 8.5 µA cm^{-2} (~ 70% of former) and 4.9 µA cm^{-2} (~ 40% of former) respectively (Fig. 3B). Thus, the current density increase for the overexpression strain was somewhat lower in the PCA-BES, which supports our earlier finding that the PYO enzymatic reduction was faster and more efficient than that with PCA (Fig. 2). The decrease in current density observed in all the BES after the peak current was reached, was primarily due to a slower substrate conversion rate (Table 1) under sustained passive aeration, but also for PYO because of degradation of this phenazine over time. PCA with a half-life of more than 10 days appeared more stable than PYO, which half-life was about one day (Fig. 4).

More detailed analyses of glucose metabolism and the products of the direct glucose oxidation showed a correlation with the peak currents. The specific glucose consumption was highest for the first two days of active aeration, with rates being the lowest for the Gcd mutant and highest for the overexpression strain (Table 1). The initial higher glucose conversion rate especially for the overexpression but also the wild-type strains in both PCA- and PYO-BES could be linked to the utilization of the periplasmic pathway for glucose oxidation. This was

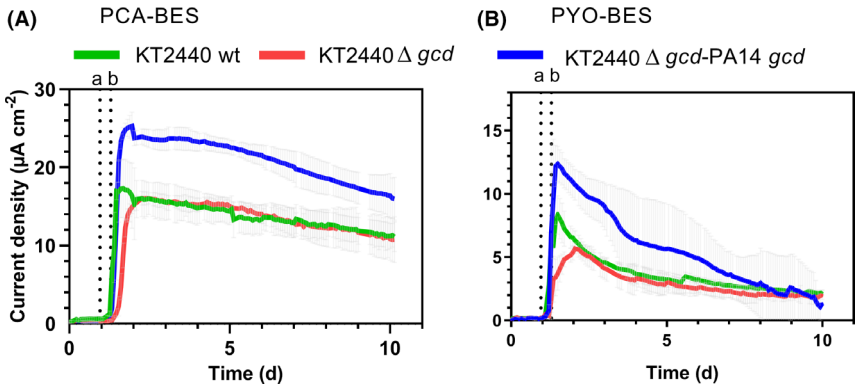

Fig. 3. Electrical current generation in a bioelectrochemical system (BES) of *P. putida* KT2440 using glucose as substrate and phenazines as electron mediators to the anode. Wild type (KT2440 wt), glucose dehydrogenase deletion mutant (KT2440 Δ*gcd*) and a glucose dehydrogenase overexpression strains of *P. putida* KT2440 (KT2440 Δ*gcd* –PA14 *gcd*) were cultivated over a period of 10 days. a: phenazines were added after 23 h of cultivation; b: active supply of oxygen was turned off after 31 h allowing only a limited amount of oxygen through a 0.2 µm sterile filter (passive aeration).
A. Current density produced using 80 mg l^{-1} PCA as electron mediator; (B) current density produced using 18 mg l^{-1} PYO as electron mediator. Results are the average of three replicates; errors bar are the SD.

Table 1. Specific glucose consumption and maximum biomass yield of *P. putida* KT2440 strains in BES using PCA or PYO as electron mediators.

	PCA- BES			PYO- BES		
Strain	Coulombic efficiency (%)	Specific glucose consumption (g l^{-1} h^{-1})[a]	Maximum biomass yield (gDCW $gGlc^{-1}$)	Coulombic efficiency (%)	Specific glucose consumption (g l^{-1} h^{-1})[a]	Maximum biomass yield (gDCW $gGlc^{-1}$)
KT2440 wt	4.06	0.09 ± 0.01	0.17 ± 0.01	0.76	0.14 ± 0.03	0.16 ± 0.04
KT2440 Δ*gcd*	5.02	0.05 ± 0.001	0.16 ± 0.01	0.81	0.1 ± 0.02	0.18 ± 0.01
KT2440 Δ*gcd*–PA14 *gcd*	8.84	0.139 ± 0.02	0.16 ± 0.02	1.27	0.17 ± 0.06	0.18 ± 0.02

a. Specific glucose consumption was calculated for the first 2 days of the BES experiment.

confirmed by the presence of gluconate and 2-ketogluconic acids in the supernatant (Fig 4). The amount of gluconate and 2-ketogluconic acids were expectedly low (about 0.2 g l^{-1}) in the wild type (Fig. 4A and B), since the rate of gluconate uptake in *P. putida KT2440* is well matched to glucose oxidation with a negligible amount going all the way to 2-ketogluconate (Nikel *et al*., 2015). The initial difference in the current density (after turning down the aeration) for both phenazines between the wild type and the mutant confirmed a contribution of the periplasmic pathway (Fig. 4C and D). It seems like phenazines can only access electrons and enable current production with a delay in the absence of Gcd. Meanwhile, the products of the periplasmic pathway were found accumulated in a high amount in the overexpression strain (Fig. 4E and F). In the PCA-BES, almost 95% of the glucose converted by the overexpression strain was found as gluconate and 2-ketogluconic acid after 2 days, showing that the sugar oxidation pathway was greatly accelerated by the overexpression; however, sugar acid uptake into the cytosol could not match their production. The effect was similar for this strain in the PYO-BES, although only 42% of the glucose was found as intermediate products of direct glucose oxidation. The correlation between the metabolic flux increase of the overexpression strain in the glucose oxidation pathway and the increased electron discharge with this strain to the BES anode strongly suggests that the direct glucose oxidation pathway indeed is an important interaction point for phenazines to mediate electrons to the anode. However, if electrons are discharged at this point, no energetic gain for the cell is possible, since the electrons will be diverted away from the electron transport chain, which drives ATP-production. To quantitatively compare the efficiency of the electron discharge via phenazines, the coulombic efficiency was calculated for the three strains. It gives the fraction of the electrons from glucose oxidation, which was mediated to the anode for current generation via the phenazines. For the PCA-BES, this value is 4.1%, 5.0% and 8.8% for the wild-type; Gcd mutant, and the overexpression strain, respectively, while it was expectedly lower in PYO-BES

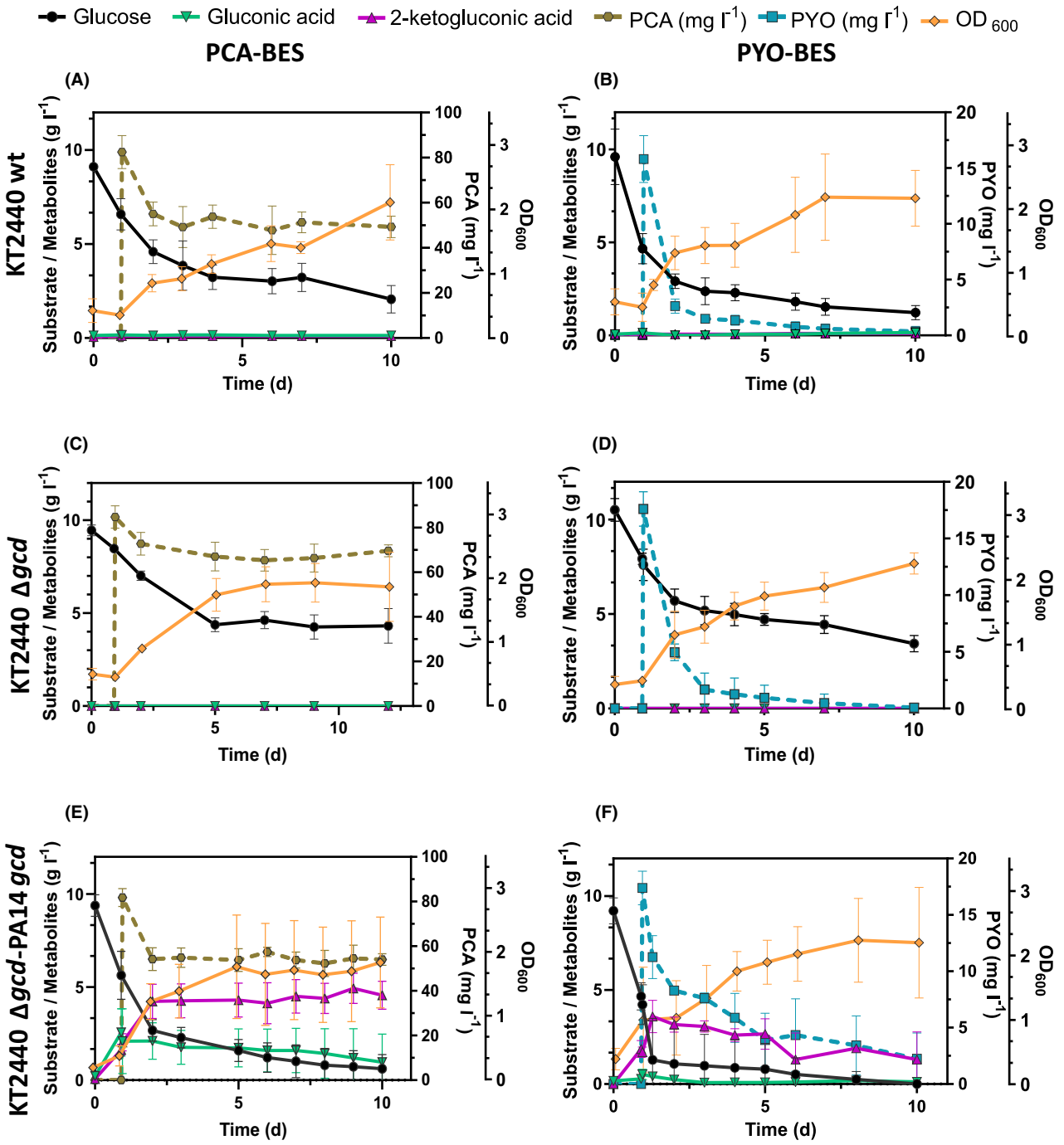

Fig. 4. Metabolic and growth (OD_{600}) profile and the stability of phenazines as electron mediator in the BES over a period of 10 days using *P. putida* KT2440. About 10 g l^{-1} glucose was used as the sole source of energy and electrons, while PCA (80 mg l^{-1}) or PYO (18 mg l^{-1}) served as electron mediators.
A. and (B) KT2440 wt; (C) and (D) KT2440 Δ*gcd*; (E) and (F) KT2440 Δ*gcd* –PA14 *gcd*. Results are the average of three replicates and errors bar are the SD.

with 0.8%, 0.8% and 1.3%, because the current was not sustained due to the instability of PYO. A higher columbic efficiency of the overexpression strain is in agreement to the high current density obtained for this strain in comparison with the other strains and to the less complete oxidation of the glucose with accumulated intermediates (Fig. 4E and F). It should be highlighted that a coulombic efficiency of almost 9% is the highest ever

observed for phenazine-based electron discharge with *Pseudomonas* (Askitosari *et al*., 2019).

Assessing the transfer capacity of phenazines across the cell membrane into the cytosol

The finding that the Gcd mutant could still generate current using the phenazines, even though it is not able to utilize the periplasmic direct glucose oxidation pathway, made it likely that phenazines also have access to electrons released in cytoplasmic metabolic pathways. Therefore, we developed two molecular biosensors to ascertain if phenazines, after initial release when synthesized or when externally added to the cell, could (re-) enter the cytoplasm (Fig. 5). The first biosensor was made to track PCA and was based on the two reaction steps that modify PCA to PYO catalysed by the two enzymes PhzM, a methyltransferase, and PhzS, a monoxygenase (Mavrodi *et al*., 2001). The genes encoding PhzM and PhzS were expressed via a plasmid in KT2440 and a PA14 mutant strain, lacking the PCA biosynthetic genes (*P. aeruginosa* PA14 Δ*phz1,2*) (Schmitz and Rosenbaum, 2020). Since neither organism can produce phenazines, but now house the cytosolic enzymes PhzM and PhzS, it is expected that externally added PCA would be transformed to PYO, only if PCA has access to the cytoplasm (Fig. 5A). Both biosensors (PA14 Δ*phz1,2-MS* and KT2440-*MS*) converted externally added PCA (40 mg l^{-1}) to about 8 mg l^{-1} PYO after 3 h (Fig. 6A). Less than 2 mg l^{-1} PYO was detected in an *in vitro* PCA reduction assay using just the supernatant of the biosensor culture, which had been induced but was never supplied with PCA. This confirmed that majority of PCA conversion occurred in the cytoplasm and was not a result of secreted enzymes or lysed cells.

Next, we designed a biosensor, which could enable us to evaluate whether PYO has access to the cytoplasm (Fig. 5B). PYO has been shown to activate the constitutively expressed transcription factor SoxR by a reversible one-electron oxidation of its [2Fe-2S] cluster (Dietrich *et al*., 2006; Sheplock *et al*., 2013; Tschirhart *et al*., 2017). This activation in *P. aeruginosa* induces the expression of proteins including the MexGHI-OpmD efflux pump operon, which likely is involved in phenazine export (Palma *et al*., 2005). We constructed the promoter of this operon (pMexG) from PA14, which preceded a *gfp* reporter gene in a plasmid and transformed it to PA14 Δ*phz1,2* and KT2440 to generate biosensors (PA14 Δ*phz1,2*-pMexG Gfp and KT2440-pMexG Gfp) in which the respective native SoxR can serve as a redox-sensing regulator for *gfp* expression (Fig. 5B).

Biosensors induced with PYO showed more Gfp fluorescence as compared to the un-induced or those induced with PCA (Fig. 6B). Un-induced biosensors, however, showed some fluorescence (Figs 6B and 7), which might be a result of superoxide ions generated during aerobic growth, which are able to activate SoxR although such oxidation is less effective in *P. aeruginosa* (Fujikawa *et al*., 2012). Inability of PCA to yield significant fluorescence compared to the un-induced biosensor could be a result of its low redox potential, since SoxR is only activated by phenazines of high redox potential (Sheplock *et al.,* 2013; Sakhtah *et al*., 2016). Although SoxR in *P. aeruginosa* and *P. putida* have a similar DNA binding domain (Park *et al*., 2006; Sheplock *et al*., 2013), the PYO-induced KT2440 biosensor shows a comparatively lower fluorescence in respect to its PA14 counterpart. This may be due to the fact that KT2440 SoxR was unable to completely activate the pMexG promoter, since the respective operon is not part of its native target regulon (Park *et al*., 2006).

Overall, both biosensors independently show that PCA and PYO, once released from the cell after synthesis, are able to re-enter the cytoplasm and therefore are able to access the diverse enzymatic reactions, for which an interaction with phenazines has already been described *in vitro* (Glasser *et al*., 2017; Jo *et al*., 2020).

Discussion

The low electron discharge efficiency of phenazines to the anode of a BES and the poor understanding of the physiology of phenazine electron transport presents a challenge for further developing an oxygen-limited bioprocess that would be supported by phenazine electron mediation. We anticipated that if periplasmic redox enzymes interact with phenazines, improving such interaction could increase the electron flux to the anode, as it has been observed for the synthetic redox mediator ferricyanide (Yu *et al*., 2018) with which highly efficient glucose oxidation to 2-ketogluconate was coupled to anodic electron discharge. Here, we have confirmed that the periplasmic PQQ-dependent glucose dehydrogenase (Gcd) is able to reduce PCA and PYO. PCA, the precursor of PYO, had an about 60-fold lower enzymatic reduction rate than PYO (Fig. 2). The reason might be their structural difference or their different redox properties ($E^{\circ\prime}$[PCA]=−0.24 V; $E^{\circ\prime}$[PYO]=−0.18 V vs. $Ag/AgCl_{sat.}$) (Bosire *et al*., 2016). The different functional groups surrounding the core phenazine structure have been shown to affect both, the chemical properties such as partitioning coefficients and the redox potentials of the individual derivatives (Bellin *et al*., 2014). Nevertheless, the longer half-life exhibited by PCA in BES operations resulted in a better performance over time compared to PYO (Fig. 3). Hence, PCA is better suited if long-term phenazine electron mediation is desired. Since phenazine electron discharge in *Pseudomonas* is not

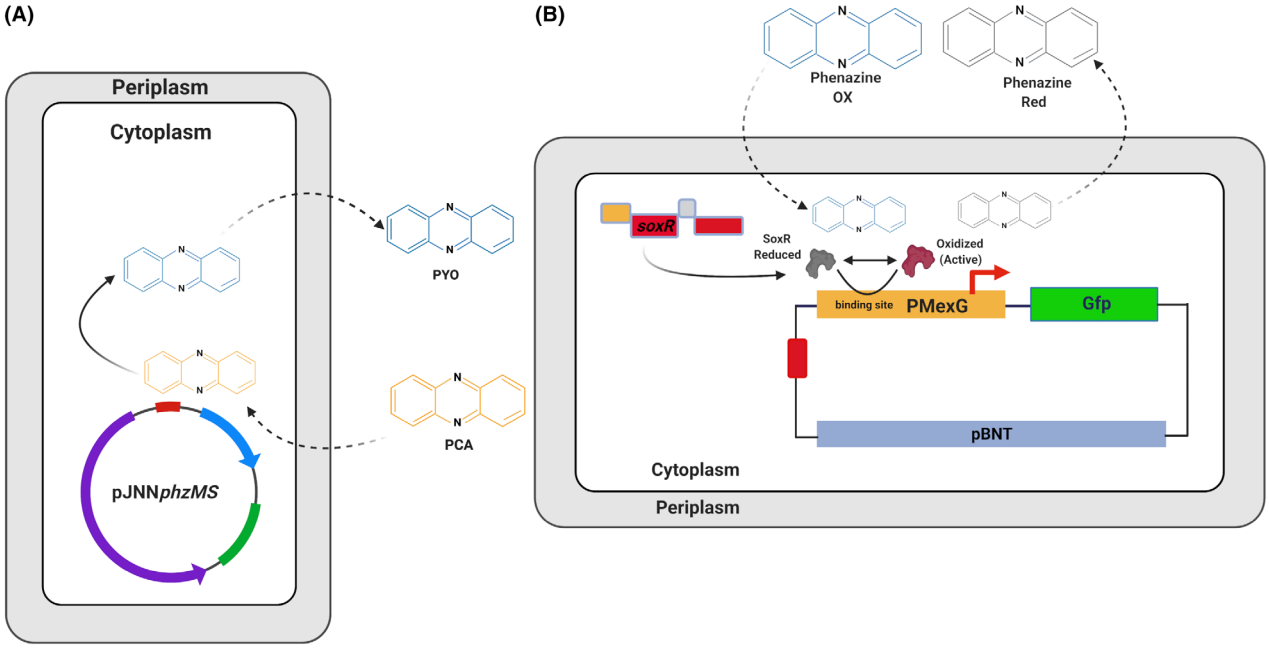

Fig. 5. Schematic illustration of the biosensor for evaluating phenazine ability to re-enter the cell once they are released.
A. detects PCA ability to enter the cytoplasm through the conversion of externally added PCA to PYO by the gene products of *phzM* and *phzS*.
B. detects phenazine (especially PYO) ability to enter the cytoplasm via the oxidation of SoxR by the phenazines, which subsequently activates the promoter of the MexGHI efflux pump (pMexG) inducing *gfp* expression.

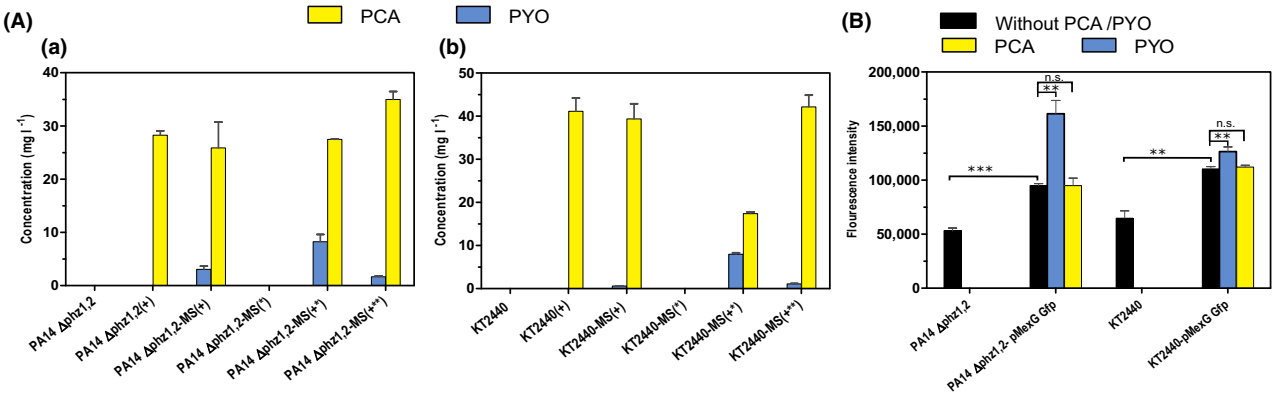

Fig. 6. Detection of phenazine ability to enter the cytoplasm of *P. aeruginosa* PA14 and *P. putida* KT2440 using cellular biosensors.
A. Biosensors which convert PCA to PYO if the former enters the cytoplasm.
(a) *P. aeruginosa* PA14 Δ*phz1,2* (phenazine knockout, control strain) and PA14 Δ*phz1,2-MS* (biosensor); (b) *P. putida* KT2440 (wild type, control strain) and KT2440-MS (biosensor) were tested. Cells were grown to OD 1 before addition of PCA (40 mg l^{-1}) and induced with 0.1 mM sodium salicylate and were further cultivated for 3 h. (+) added PCA, (*) induction by sodium salicylate, (+*) added PCA and induction by sodium salicylate, and (+**) PCA was added to the supernatant of induced biosensors strain and incubated for 1 h at 37°C. (B) Biosensors for the detection of intracellular PYO – based on a PYO-regulated promotor controlling Gfp fluorescence. The *gfp* gene was cloned behind the promoter of the *P. aeruginosa* PA14 efflux protein MexGHI-OpmD (pMexG), which is activated when phenazines oxidize the redox regulator SoxR. *P. aeruginosa* PA14 Δ*phz1,2*-pMexG-*gfp* (biosensor) and *P. putida* KT2440-pMexG-*gfp* (biosensor) and their respective controls were induced after 3 h for the expression of Gfp with 4 mg l^{-1} (20 μM) PYO or 9 mg l^{-1} (40 μM) PCA and cultivated for 16 h. The fluorescence of the control strains shows the auto-fluorescence of the organism. Fluorescence of the Gfp construct without phenazine addition shows untargeted induction of the pMexG promotor, for example by other redox-active compounds. Unpaired t-test was used to compare the fluorescence of Gfp and is represented as (**$P < 0.01$; ***$P < 0.001$ and n.s.-no statistical significance-$P > 0.05$). Results are average of three replicates, and error bars represent the SD.

limited to glucose as a substrate, we also investigated other PQQ-dependent periplasmic enzymes. The alcohol substrates 2,3-butanediol and ethanol also show anodic current production (Bosire *et al.*, 2016) and can be metabolized by the periplasmic PQQ-dependent ethanol dehydrogenase (Edh). However, the *in vitro* assay of this

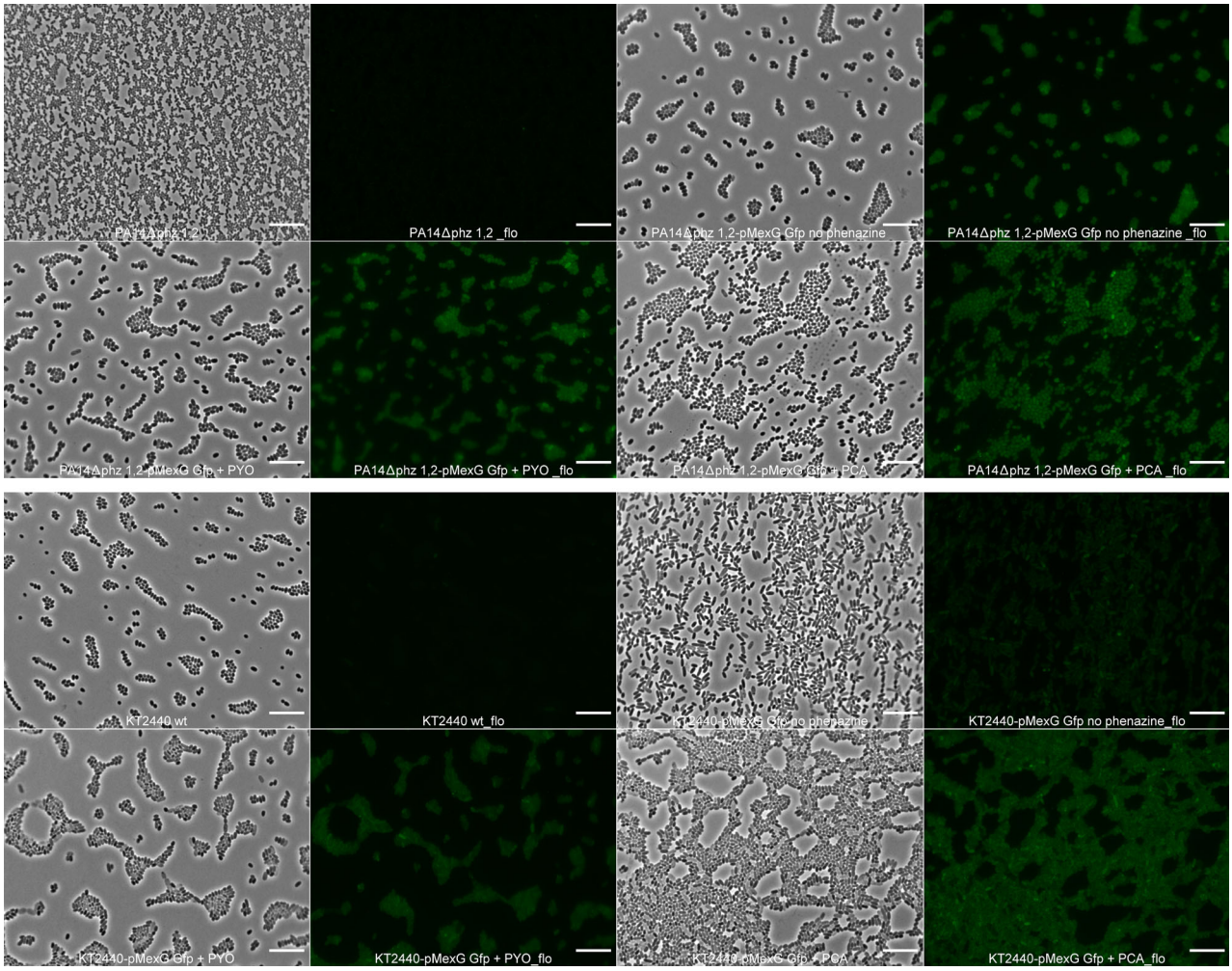

Fig. 7. Microscopy images of the parent and biosensor strains for evaluating phenazine cytoplasmic access. Bright field and the corresponding fluorescent microscopy of the strains used to track phenazine access to the cytoplasm through the expression of Gfp. Scale bar: 10 μm.

enzyme showed no reduction of PCA or PYO with either of the alcohols (data not shown). In contrast, the artificial electron acceptor DCPIP was reduced in this assay, showing functionality of the Edh enzyme. The PQQ-dependent enzyme reaction is believed to use the same (hydrid) transfer mechanism for both alcohol (Edh) and aldehyde (Gcd) dehydrogenases (Anthony, 1996; Oubrie *et al*., 1999). Nonetheless, factors such as differences in the charged amino acid residues around the substrate entrance pocket might still influence electron acceptor preference (Hiraka *et al*., 2020). The mode of extracellular electron transfer achieved *in vivo* using phenazines or other redox mediators, however, does not only depend on the enzymes, which directly catalyse the reduction of these mediators. Other respiratory components of the cell, such as menaquinone, cytochrome reductase and terminal oxidases, were recently shown to play a critical role in the reduction of these mediators (Feng *et al*., 2020; Jo *et al*., 2020; Lai *et al*., 2020). However, the delay experienced in attaining peak currents with the Gcd mutant strain in addition to the improved current from the overexpression strain point to a central role of periplasmic Gcd for phenazine-based electron discharge. Further research is now required to elucidate a possible connection of the Gcd-phenazine interaction to the reported components of the electron transport chain.

While our results from the periplasmic enzyme investigation in the BES showed a strong involvement of the glucose oxidation pathway in phenazine charging, they also showed that even when this pathway is abolished in the Gcd mutant strain, electrons are transferred to phenazines. If glucose cannot be oxidized in the periplasm, it is directly taken up into the cytoplasm and phosphorylated by a glucokinase (Nikel *et al*., 2015). Although several cytoplasmic enzymes have been shown to be able to reduce phenazines (Glasser *et al*.,

2017; Jo *et al*., 2020), it was not clear if phenazines could re-enter the cytoplasm once they were released after their synthesis. Since phenazines themselves are also toxic, *Pseudomonas aeruginosa* uses different mechanisms such as a MexGHI-OpmD efflux pump and PumA, a monoxygenase, for self-resistance (Sakhtah *et al*., 2016; Sporer *et al*., 2018). While the efflux pump is speculated to be involved in phenazine expulsion, no putative entry pathway has been proposed yet. A direct observation of the phenazine transfer across the cell membrane is difficult due to the lack of labelling strategies for phenazines. Instead, with the aid of molecular biosensors, we here show that both phenazines can have access to the cytoplasm once released and consequently access the electron pool in this part of the cell.

However, taking all presented experiments together; the sustainability of extracellular current production in the Gcd deletion mutant, the established uptake of PCA and the probable uptake of PYO into the cytoplasm; it is not clear yet, why this access to metabolic electrons is so limited, that is does not translate to higher coulombic efficiencies. Potentially, several central enzymes of the glucose catabolism should be able to reduce phenazines, diverting electrons away from the native electron transport chain for oxygen reduction. Moreover, the fact that phenazine reduction is influenced by components of the electron transport chain (Jo *et al*., 2020), gives further indication that there must be mechanism to prevent cytosolic enzymes from reducing phenazines. This makes sense from an energetic point of view, because phenazine reduction by catabolic enzymes would result in the loss of reducing equivalents without energy conservation. Therefore, a better understanding of the control or synergy between catabolic enzyme catalysed phenazine reduction and reduction of phenazine by components of the respiratory chain would provide a wider view to understand and improve phenazine extracellular electron transfer. With this next level of insight, finally an answer could be found to the question if and how phenazine-based electron discharge can or could be coupled to cellular ATP generation.

Experimental procedures

Microorganisms, plasmids and culture conditions

Details on all strains and plasmids used for this study are listed in supporting Table S1.

All *E. coli* strains were grown in lysogeny broth (LB) containing 50 $\mu g\ ml^{-1}$ kanamycin (km) at 37°C. For enzyme purification, *E. coli* expressing the gene for Gcd were grown in a 4-L batch using a Biostat® B-DCU bioreactor (B. Braun Biotech International GmbH, Melsungen Germany) as detailed in the Data S1. *P. aeruginosa* PA14 and *P. putida* KT2440 were initially cultivated in LB at 37°C and 30°C respectively. For all experiment with *P. aeruginosa* PA14, MOPS medium was prepared according to (Neidhardt *et al*., 1974) with 3.5 $g\ l^{-1}$ glucose as carbon source. 50 $\mu g\ ml^{-1}$ km was used as antibiotic and 0.1 mM sodium salicylate was used to induce the plasmids when required. For the biosensor experiment, a 10 ml culture was cultivated until an optical density of 1, after which PCA was added and cells were induced when necessary. MOPS medium was also used for the *P. putida* KT2440 biosensor experiment converting PCA to PYO because it was easier to keep the pH stable. All other experiments with *P. putida* KT2440 were performed in a Delft mineral salt medium, which contained per litre: 10 g glucose, 3.88 g K_2HPO_4, 1.63 g NaH_2PO_4, 2 g $(NH_4)_2SO_4$, 0.1 g $MgCl_2 \cdot 6\ H_2O$, 10 mg EDTA, 2 mg $ZnSO_4 \cdot 7H_2O$, 1 mg $CaCl_2 \cdot 2H_2O$, 5 mg $FeSO_4 \cdot 7H_2O$, 0.2 mg $Na_2MoO_4 \cdot 2\ H_2O$, 0.2 mg $CuSO_4 \cdot 5\ H_2O$, 0.4 mg $CoCl_2 \cdot 6\ H_2O$ and 1 mg $MnCl_2 \cdot 2\ H_2O$. The pH of the BES bioreactors was maintained above 6.0 using 2 N NaOH.

Heterologous enzyme expression and purification

The molecular constructs for the overexpression of the *gcd* gene of *P. aeruginosa* PA14 and *P. putida* KT2440 in *E. coli* BL21 (DE3), the *gcd* gene of *P. aeruginosa* PA14 in *P. putida* KT2440 Δ*gcd*, the enzyme production and purification protocols as well as the molecular construction of the biosensors are explained in detail in the Data S1.

Enzyme assay

Activity of the Gcd enzymes for phenazine reduction was assessed with a modified PQQ-dependent reductase assay as described in Mennenga *et al*. (2009). In the original assay, the electrons released during glucose oxidation are transferred from the PQQ co-factor to the synthetic redox mediator PMS and finally to the non-reversible chromophore electron acceptor DCPIP. In our modified version, the synthetic electron acceptor system (PMS + DCPIP) was replaced by either PCA or PYO and their reduction was followed spectrometrically. The concentration of the protein used for activity measurement was determined using the Bradford method (Bradford, 1976). Then, all components of the enzyme assay were first gassed with nitrogen for about 30 min to ensure anaerobic conditions, as oxygen easily re-oxidizes the phenazines and therefore hampers the measurement. The reaction mixture was prepared in an anaerobic chamber (Coy Lab products, Grass Lake, MI, USA) prior to measurement outside in a CLARIOstar plate reader (BMG Labtech, Orteberg, Germany), which was constantly flushed with nitrogen resulting in a

reduced oxygen environment of 1.2%. The assay mixture contained a final volume of 200 μl (100 mM Tris-HCl, pH 7.1; 1 mM $CaCl_2$, 5 μM PQQ, 0.45 mM phenazine (PYO or PCA), 65 μg purified enzyme and 20 mM glucose). All assay components, except glucose, were first mixed and incubated at 30°C for 30 min before glucose was added as a substrate or an equivalent volume of water as a control, to start the reaction. Remaining oxidized PYO was measured at 690 nm, while accumulated reduced PCA was measured at 440 nm. Since PCA is re-oxidized by oxygen very fast even though the enzymatic reduction is slow, the microtiter plate containing the assay mixture with PCA was kept in an anaerobic chamber and only brought out at intervals for plate reader measurements. Extinction coefficients used were $\varepsilon_{440} = 2.206\ mM^{-1}cm^{-1}$ for reduced PCA (Glasser *et al.*, 2017) and $\varepsilon_{690} = 4.5\ mM^{-1}\ cm^{-1}$ for oxidized PYO (determined in this work, see Fig. S2).

Bioelectrochemical systems set-up and procedures

BES set-up (see Fig. S3) and operation were identical as reported previously (Askitosari *et al.*, 2019). The BES reactor was made of a single-chamber 500-ml (working volume) glass reactor with a water jacket for temperature control (Laborglas Lammek, Moers, Germany). It contained a three-electrode set-up: a working electrode (anode) made of a carbon comb - $7.3 \times 4.7 \times 0.9$ cm (geometrical surface area = 156.32 cm^2) attached to a graphite rod, a counter electrode (cathode) - $7.3 \times 2.2 \times 0.9$ cm carbon block (49.22 cm^2) attached to a graphite rod and a reference electrode (RE) – Ag/AgCl, saturated with KCl (192 mV vs. SHE at 30°C). All carbon materials were of high-grade graphite (EDM-3, Novotec, Nettetal, Germany). Butyl rubber gaskets were used to seal all ports for the electrodes, gas-in/out and sampling.

The BES reactors were operated with a VMP-300 potentiostat (BioLogic Science Instruments, Seyssinet-Pariset, France). Experiments were performed at 30°C and stirred at 200 rpm with a magnetic stirrer. Chronoamperometry measurement of the electric current was recorded at a set potential of 0.2 V against RE. Electric current of the blank medium was first recorded for 24 h before inoculation, and thereafter, the recording was interrupted every 22 h for a 2 h cyclic voltammetry measurement (data not shown). Sampling for determination of the optical density at 600 nm, pH and metabolites production was performed at regular intervals. Experiments were performed under two oxygen-limited conditions: initially, active aeration (AA) of the medium with an oxygen flow rate of 30 ml min^{-1} was supplied to the reactors for the first 31 hours through a sparger connected to a 0.2 μm sterile PTFE filter (DIA-Nielsen, Düren, Germany); thereafter, passive aeration (PA) was applied for the rest of the experiment that allowed air passively into the reactor headspace through a 0.2 μm sterile PTFE filter. Phenazines (80 mg l^{-1} PCA or 18 mg l^{-1} PYO) were added to the system 23 h after inoculation.

Analytical procedures

Analysis of central metabolites: Glucose was measured using a YSI 2900D Biochemistry Analyser (YSI Incorporated, Ohio, USA). Analysis of secreted metabolites was performed using a HPLC (Jasco Deutschland GmbH, Pfungstadt, Germany) with an Aminex HPX-87H 300 nm × 7.8 mm, 9 μm ion exclusion column (Bio-Rad, Hercules, CA, USA). Isocratic elution was achieved using 5 mM H_2SO_4 at a flow rate of 0.5 ml min^{-1}. Signals were detected with a UV detector (210 nm) and a refractive index (RI) detector.

Analysis of phenazines: A 1:2 dilution of the supernatant from the BES in acetonitrile was kept at 4°C overnight, to allow for protein precipitation. Thereafter, the samples were centrifuged, and the supernatant was used for measurement. Phenazines were analysed using a reverse-phase HPLC with a 250 × 4.0 mm, 5 μm column (Bischoff Chromatography, Leonberg, Germany). Elution was performed in a gradient of 0.1% trifluoroacetic acid (TFA) (v/v) in water plus 0.1% TFA (v/v) in acetonitrile with a flow rate of 1 ml min^{-1}. PCA and PYO were detected at 360 and 280 nm, respectively, with retention times of 18.1 min (PCA) and 9.0 min (PYO) and compared to standard solution of phenazines (PYO, Sigma Aldrich, Taufkirchen, Germany; PCA, Apollo Scientific, Cheshire, UK).

Calculating charge/energy balance

To determine the coulombic efficiency as the fraction of harvested electrons in relation to the charge (Q) contained in the substrate glucose in the form of reducing equivalents, the following equation was used to calculate the energy balance:

$$CE(\%) = \left(Q_{(anode)} / Q_{(glucose\ utilized)} - Q_{(sugar\ acid\ metabolites)}\right) \times 100.$$

With Q being the charge equivalent [C] accessible, which can be calculated using Faraday's Law $Q = n \cdot z \cdot F$, where: n = amount of consumed substrate [mol], z = number of transferable electrons per molecule of substrate (for glucose = 24), F = Faraday constant (96485.3 C mol^{-1}), or from the integrated anodic current $Q_{(anode)} = \int I\ (t)$, where I = anodic current [A] and t = time [s]. Anodic charge was calculated using the EC-Lab software (Biologic Science instruments, Seyssinet-Pariset, France), while charge for other terms was determined from the obtained quantitative data.

Acknowledgement

Miriam Rosenbaum has received funding from the European Research Council (ERC) under the European Union's Horizon 2020 research and innovation programme (Grant agreement No. 864669).

Funding Information

Miriam Rosenbaum has received funding from the European Research Council (ERC) under the European Union's Horizon 2020 research and innovation programme (Grant agreement No. 864669).

Conflict of interest

None declared.

References

Alexandre, G., Greer-Phillips, S., and Zhulin, I.B. (2004) Ecological role of energy taxis in microorganisms. *FEMS Microbiol Rev* **28:** 113–126.

Anthony, C. (1996) Quinoprotein-catalysed reactions. *Biochem J* **320:** 697–711.

Askitosari, T.D. (2019) *Engineering Pseudomonas putida* KT2440 for efficient bioelectrochemical production of glycolipids. PhD thesis RWTH Aachen University.

Askitosari, T.D., Boto, S.T., Blank, L.M., and Rosenbaum, M.A. (2019) Boosting heterologous phenazine production in *Pseudomonas putida* KT2440 through the exploration of the natural sequence space. *Front Microbiol* **10:** 199.

Beblawy, S., Bursac, T., Paquete, C., Louro, R., Clarke, T.A., and Gescher, J. (2018) Extracellular reduction of solid electron acceptors by *Shewanella oneidensis*. *Mol Microbiol* **109:** 571–583.

Bellin, D.L., Sakhtah, H., Rosenstein, J.K., Levine, P.M., Thimot, J., Emmett, K., *et al.* (2014) Integrated circuit-based electrochemical sensor for spatially resolved detection of redox-active metabolites in biofilms. *Nat Commun* **5:** 3256.

Blankenfeldt, W., and Parsons, J.F. (2014) The structural biology of phenazine biosynthesis. *Curr Opin Struct Biol* **29:** 26–33.

Bosire, E.M., Blank, L.M., and Rosenbaum, M.A. (2016) Strain- and substrate-dependent redox mediator and electricity production by *Pseudomonas aeruginosa*. *Appl Environ Microbiol* **82:** 5026–5038.

Bradford, M.M. (1976) A rapid and sensitive method for the quantitation of microgram quantities of protein utilizing the principle of protein-dye binding. *Anal Biochem* **72:** 248–254.

Brutinel, E.D., and Gralnick, J.A. (2012) On the role of endogenous electron shuttles in extracellular electron transfer. In *Microbial Metal Respiration: From Geochemistry to Potential Applications*. Gescher, J., and Kappler, A. (eds). Berlin: Springer, pp. 83–105.

da Silva, A.J., Cunha, J.D.S., Hreha, T., Micocci, K.C., Selistre-de-Araujo, H.S., Barquera, B., and Koffas, M.A.G. (2021) Metabolic engineering of *E. coli* for pyocyanin production. *Metab Eng* **64:** 15–25.

Daddaoua, A., Krell, T., Alfonso, C., Morel, B., and Ramos, J.-L. (2010) Compartmentalized glucose metabolism in *Pseudomonas putida* is controlled by the PtxS repressor. *J Bacteriol* **192:** 4357–4366.

Dietrich, L.E., Price-Whelan, A., Petersen, A., Whiteley, M., and Newman, D.K. (2006) The phenazine pyocyanin is a terminal signalling factor in the quorum sensing network of *Pseudomonas aeruginosa*. *Mol Microbiol* **61:** 1308–1321.

Feng, J., Lu, Q., Li, K., Xu, S., Wang, X., Chen, K., and Ouyang, P. (2020) Construction of an electron transfer mediator pathway for bioelectrosynthesis by *Escherichia coli*. *Front Bioeng Biotechnol* **8:** 590667.

Feng, J., Qian, Y., Wang, Z., Wang, X., Xu, S., Chen, K., and Ouyang, P. (2018) Enhancing the performance of *Escherichia coli*-inoculated *microbial fuel cells by introduction of the phenazine-1-carboxylic acid pathway. J Biotechnol* **275:** 1–6.

Fujikawa, M., Kobayashi, K., and Kozawa, T. (2012) Direct oxidation of the [2Fe-2S] cluster in SoxR protein by superoxide: distinct differential sensitivity to superoxide-mediated signal transduction. *J Biol Chem* **287:** 35702–35708.

Glasser, N.R., Kern, S.E., and Newman, D.K. (2014) Phenazine redox cycling enhances anaerobic survival in *Pseudomonas aeruginosa* by facilitating generation of ATP and a proton-motive force. *Mol Microbiol* **92:** 399–412.

Glasser, N.R., Wang, B.X., Hoy, J.A., and Newman, D.K. (2017) The pyruvate and alpha-ketoglutarate dehydrogenase complexes of *Pseudomonas aeruginosa* catalyze pyocyanin and phenazine-1-carboxylic acid reduction via the subunit dihydrolipoamide dehydrogenase. *J Biol Chem* **292:** 5593–5607.

Hall, S., McDermott, C., Anoopkumar-Dukie, S., McFarland, A., Forbes, A., Perkins, A., *et al.* (2016) Cellular effects of pyocyanin, a secreted virulence factor of *Pseudomonas aeruginosa*. *Toxins (Basel)* **8:** 236.

Hiraka, K., Tsugawa, W., and Sode, K. (2020) Alteration of electron acceptor preferences in the oxidative half-reaction of flavin-dependent oxidases and dehydrogenases. *Sci Int J Mol* **21:** 3797.

Jahn, B., Jonasson, N.S.W., Hu, H., Singer, H., Pol, A., Good, N.M., *et al.* (2020) Understanding the chemistry of the artificial electron acceptors PES. *PMS, DCPIP and Wurster's Blue in methanol dehydrogenase assays, JBIC* **25:** 199–212.

Jo, J., Price-Whelan, A., Cornell, W.C., and Dietrich, L.E.P. (2020) Interdependency of respiratory metabolism and phenazine-associated physiology in *Pseudomonas aeruginosa* PA14. *J Bacteriol* **202:** e00700–00719.

Kato, S. (2015) Biotechnological aspects of microbial extracellular electron transfer. *Microbes Environ* **30:** 133–139.

Kobayashi, K., Mustafa, G., Tagawa, S., and Yamada, M. (2005) Transient formation of a neutral ubisemiquinone radical and subsequent intramolecular electron transfer to pyrroloquinoline quinone in the *Escherichia coli* membrane-integrated glucose dehydrogenase. *Biochemistry* **44:** 13567–13572.

Kohlstedt, M., and Wittmann, C. (2019) GC-MS-based (13)C metabolic flux analysis resolves the parallel and cyclic

glucose metabolism of *Pseudomonas putida* KT2440 and *Pseudomonas aeruginosa* PAO1. *Metab Eng* **54:** 35–53.

Kracke, F., Vassilev, I., and Kromer, J.O. (2015) Microbial electron transport and energy conservation - the foundation for optimizing bioelectrochemical systems. *Front Microbiol* **6:** 575.

Kuypers, M.M.M., Marchant, H.K., and Kartal, B. (2018) The microbial nitrogen-cycling network. *Nat Rev Microbiol* **16:** 263–276.

Lai, B., Bernhardt, P.V., and Krömer, J.O. (2020) Cytochrome c reductase is a key enzyme involved in the extracellular electron transfer pathway towards transition metal complexes in *Pseudomonas putida*. *Chemsuschem* **13:** 5308–5317.

Logan, B.E., Rossi, R., Ragab, A.A., and Saikaly, P.E. (2019) Electroactive microorganisms in bioelectrochemical systems. *Nat Rev Microbiol* **17:** 307–319.

Lovley, D.R., and Walker, D.J.F. (2019) Geobacter protein nanowires. *Front Microbiol* **10:** 2078.

Mavrodi, D.V., Bonsall, R.F., Delaney, S.M., Soule, M.J., Phillips, G., and Thomashow, L.S. (2001) Functional analysis of genes for biosynthesis of pyocyanin and phenazine-1-carboxamide from *Pseudomonas aeruginosa* PAO1. *J Bacteriol* **183:** 6454–6465.

Mennenga, B., Kay, C.W., and Gorisch, H. (2009) Quinoprotein ethanol dehydrogenase from *Pseudomonas aeruginosa*: the unusual disulfide ring formed by adjacent cysteine residues is essential for efficient electron transfer to cytochrome c550. *Arch Microbiol* **191:** 361–367.

Mentel, M., Ahuja, E.G., Mavrodi, D.V., Breinbauer, R., Thomashow, L.S., and Blankenfeldt, W. (2009) Of two make one: the biosynthesis of phenazines. *ChemBioChem* **10:** 2295–2304.

Neidhardt, F.C., Bloch, P.L., and Smith, D.F. (1974) Culture medium for enterobacteria. *J Bacteriol* **119:** 736–747.

Nikel, P.I., Chavarría, M., Fuhrer, T., Sauer, U., and de Lorenzo, V. (2015) *Pseudomonas putida* KT2440 strain metabolizes glucose through a cycle formed by enzymes of the entner-doudoroff, embden-meyerhof-parnas, and pentose phosphate pathways. *J Biol Chem* **290:** 25920–25932.

Oubrie, A., Rozeboom, H.J., Kalk, K.H., Olsthoorn, A.J.J., Duine, J.A., and Dijkstra, B.W. (1999) Structure and mechanism of soluble quinoprotein glucose dehydrogenase. *EMBO J* **18:** 5187–5194.

Palma, M., Zurita, J., Ferreras, J.A., Worgall, S., Larone, D.H., Shi, L., *et al*. (2005) *Pseudomonas aeruginosa* SoxR does not conform to the archetypal paradigm for SoxR-dependent regulation of the bacterial oxidative stress adaptive response. *Infect Immun* **73:** 2958–2966.

Pandey, P., Shinde, V.N., Deopurkar, R.L., Kale, S.P., Patil, S.A., and Pant, D. (2016) Recent advances in the use of different substrates in microbial fuel cells toward wastewater treatment and simultaneous energy recovery. *Appl Energy* **168:** 706–723.

Pant, D., Singh, A., Bogaert, G.V., Olsen, S.I., Nigam, P.S., Diels, L., and Vanbroekhoven, K. (2012) Bioelectrochemical systems (BES) for sustainable energy production and product recovery from organic wastes and industrial wastewaters. *RSC Adv* **2:** 1248–1263.

Park, W., Peña-Llopis, S., Lee, Y., and Demple, B. (2006) Regulation of superoxide stress in *Pseudomonas putida* KT2440 is different from the SoxR paradigm in Escherichia coli. *Biochem Biophys Res Commun* **341:** 51–56.

Pham, T.H., Boon, N., De Maeyer, K., Hofte, M., Rabaey, K., and Verstraete, W. (2008) Use of Pseudomonas species producing phenazine-based metabolites in the anodes of microbial fuel cells to improve electricity generation. *Appl Microbiol Biotechnol* **80:** 985–993.

Price-Whelan, A., Dietrich, L.E.P., and Newman, D.K. (2007) Pyocyanin alters redox homeostasis and carbon flux through central metabolic pathways in *Pseudomonas aeruginosa* PA14. *J Bacteriol* **189:** 6372–6381.

Sakhtah, H., Koyama, L., Zhang, Y., Morales, D.K., Fields, B.L., Price-Whelan, A., *et al*. (2016) The *Pseudomonas aeruginosa* efflux pump MexGHI-OpmD transports a natural phenazine that controls gene expression and biofilm development. *PNAS* **113:** E3538–3547.

Saunders, S.H., Tse, E.C.M., Yates, M.D., Otero, F.J., Trammell, S.A., Stemp, E.D.A., *et al*. (2020) Extracellular DNA promotes efficient extracellular electron transfer by pyocyanin in *Pseudomonas aeruginosa* biofilms. *Cell* **182:** 919–932.e919.

Van Schie, B.J., Hellingwerf, K.J., Van Dijken, J.P., Elferink, M.G., Van Dijl, J.M., Kuenen, J.G., and Konings, W.N. (1985) Energy transduction by electron transfer via a pyrrolo-quinoline quinone-dependent glucose dehydrogenase in *Escherichia coli*, *Pseudomonas aeruginosa*, and *Acinetobacter calcoaceticus* (var. lwoffi). *J Bacteriol* **163:** 493–499.

Schmitz, S., Nies, S., Wierckx, N., Blank, L.M., and Rosenbaum, M.A. (2015) Engineering mediator-based electroactivity in the obligate aerobic bacterium *Pseudomonas putida* KT2440. *Front Microbiol* **6:** 284.

Schmitz, S., and Rosenbaum, M.A. (2020) Controlling the production of pseudomonas phenazines by modulating the genetic repertoire. *ACS Chem Biol* **15:** 3244–3252.

Sheplock, R., Recinos, D.A., Mackow, N., Dietrich, L.E.P., and Chander, M. (2013) Species-specific residues calibrate SoxR sensitivity to redox-active molecules. *Mol Microbiol* **87:** 368–381.

Shi, L., Dong, H., Reguera, G., Beyenal, H., Lu, A., Liu, J., *et al*. (2016) Extracellular electron transfer mechanisms between microorganisms and minerals. *Nat Rev Microbiol* **14:** 651–662.

Sporer, A.J., Beierschmitt, C., Bendebury, A., Zink, K.E., Price-Whelan, A., Buzzeo, M.C., *et al*. (2018) *Pseudomonas aeruginosa* PumA acts on an endogenous phenazine to promote self-resistance. *Microbiology* **164:** 790–800.

Tschirhart, T., Kim, E., McKay, R., Ueda, H., Wu, H.-C., Pottash, A.E., *et al*. (2017) Electronic control of gene expression and cell behaviour in *Escherichia coli* through redox signalling. *Nat Commun* **8:** 14030.

Van Schie, B.J., Hellingwerf, K.J., Van Dijken, J.P., Elferink, M.G., Van Dijl, J.M., Kuenen, J.G., and Konings, W.N. (1985) Energy transduction by electron transfer via a pyrrolo-quinoline quinone-dependent glucose dehydrogenase in *Escherichia coli*, *Pseudomonas aeruginosa*, and *Acinetobacter calcoaceticus* (var. lwoffi). *J Bacteriol* **163:** 493–499.

Wang, Y., Kern, S.E., and Newman, D.K. (2010) Endogenous phenazine antibiotics promote anaerobic survival of *Pseudomonas aeruginosa* via extracellular electron transfer. *J Bacteriol* **192:** 365–369.

Yang, Z.-S., Ma, L.-Q., Zhu, K., Yan, J.-Y., Bian, L., Zhang, K.-Q., and Zou, C.-G. (2016) Pseudomonas toxin pyocyanin triggers autophagy: implications for pathoadaptive mutations. *Autophagy* **12:** 1015–1028.

Yu, S., Lai, B., Plan, M.R., Hodson, M.P., Lestari, E.A., Song, H., and Krömer, J.O. (2018) Improved performance of *Pseudomonas putida* in a bioelectrochemical system through overexpression of periplasmic glucose dehydrogenase. *Biotechnol Bioeng* **115:** 145–155.

Supporting information

Additional supporting information may be found online in the Supporting Information section at the end of the article.

Fig. S1. SDS PAGE showing the purified membrane-bound glucose dehydrogenase (Gcd) of *P. putida* KT2440 and *P. aeruginosa* PA14.

Fig. S2. Determination of the extinction coefficient (ε_{690}) in mM^{-1} cm^{-1} of oxidized PYO.

Fig. S3. Photography of the BES setup.

Table S1. Strains and plasmids used for this study.

Table S2. Primers used in this study.

Data S1. Heterologous enzyme expression and purification.

